An X-Band Spacecraft Transponder for Deep Space Applications—Design Concepts and Breadboard Performance

Narayan R. Mysoor, *Senior Member, IEEE*, Jonathan D. Perret, *Member, IEEE*, and Arthur W. Kermode, *Member, IEEE*

Abstract—**This article summarizes the design concepts and measured performance characteristics of an *X*-band breadboard deep-space transponder (DST) for future spacecraft applications, with the first use scheduled for the Cassini missions in 1997 and 1996, respectively. The DST consists of a double-conversion, superheterodyne, automatic phase tracking receiver, and an *X*-band exciter to drive redundant downlink power amplifiers. The receiver acquires and coherently phase tracks the modulated or unmodulated *X*-band uplink carrier signal. The exciter phase modulates the *X*-band downlink signal with composite telemetry and ranging signals. The measured tracking threshold, automatic gain control (AGC), static phase error, and phase jitter characteristics of the breadboard DST are in good agreement with the expected performance. The measured results show a receiver tracking threshold of −158 dBm and a dynamic signal range of 88 dB.**

I. Introduction

TELECOMMUNICATION transponders [1] for deep-space spacecraft applications provide independent uplink command and turnaround ranging functions, as well as downlink telemetry and radiometric capabilities. The spacecraft DST is an element in the overall deep space communications system. The DST functions include:

1) Precise phase/frequency reference transfer from the uplink signal.

2) Demodulation of the command and ranging signals from the uplink carrier.

3) Generation of a coherent or noncoherent downlink tracking signal for the Earth-based Deep Space Network.

4) Modulation of downlink signal with composite telemetry data and turnaround ranging or differential one-way ranging (DOR) signals.

5) Capable of utilizing an external ultrastable oscillator (USO) to generate the downlink signal.

6) Generation of phase coherent reference signals for use by external *S*-band and *Ka*-band exciters.

This article describes the design, implementation, and performance of a breadboard DST configuration. The design specifications and functional description of the DST are summarized in Section II. The DST block diagram is described in Section III. The experimental results of a breadboard DST are presented in Section IV. Finally, some conclusions are drawn in Section V. Derivations of carrier tracking threshold, and phase jitter are included in an Appendix.

Manuscript received May 8, 1991; revised November 6, 1991.

The authors are with the Jet Propulsion Laboratory, California Institute of Technology, 4800 Oak Grove Drive, Pasadena, CA 91109.

IEEE Log Number 9107457.

II. Key Design Requirements

The design requirements for the DST [2] are summarized in Table I. In addition to the DST functions described in the previous section, carrier acquisition, tracking, navigation, Doppler accuracy, and radio science requirements are some of the system considerations that determine the DST specifications. The DST is to provide a receive and transmit capability at *X*-band with the necessary reference signals for generation of independent *S*-band and *Ka*-band downlink signals external to the DST. The design ratio of transmit/receive frequency translation for DST coherent operation at *X*-band is 880/749. The DST received uplink is at an assigned channel in the frequency range from 7145 to 7190 MHz ($749F_1$). The term F_1 represents the frequencies ranging from 9.54238 MHz to 9.60108. It also represents 1/12th of the voltage controlled oscillator (VCO) frequency when the receiver loop is in lock. The frequency F_1 for channel number 14 is equal to 9.5625 MHz. The DST *X*-band ($880F_1$) downlink frequency for the corresponding frequency channel assignment is in the frequency range from 8400 to 8450 MHz (Table I). The receiver performance requirements include a typical noise figure of 1.4 dB, a tracking threshold level of −157.3 dBm, and a tracking range of ±250 kHz at the assigned channel frequency. The acquisition and tracking rate is specified to be at least 550 Hz/sec. The specified nominal output power of the exciter is +12 dBm. The exciter output is phase modulated to a maximum phase deviation of ±2.5 radians with a radio frequency (RF) modulation bandwidth greater than 40 MHz. The phase noise as measured from 5 Hz to 25 MHz is required to be less than 2.5° root mean square (rms) in the coherent mode and 2.8° rms in the noncoherent mode. The DST ranging and carrier phase delay variations are to be less than 22 nsec and 2.5 nsec over the temperature

TABLE I
DEEP-SPACE TRANSPONDER (DST) SPECIFICATIONS

Parameter	Design requirements
1. Uplink frequency allocation	7145 to 7190 MHz, deep space
2. Downlink frequency allocation	8400 to 8450 MHz, deep space
3. Frequency translation ratios	
Channel 14 uplink frequency	7162.3125 MHz ($749F_1$)
X-band downlink	880/749 (8415 MHz)
S-band downlink	240/749 (2295 MHz)
Ka-band downlink	3344/749 (31977 MHz)
4. Receiver parameters	
Carrier threshold	−157.3 dBm
Dynamic range	88 dB (carrier threshold to −70 dBm)
Noise figure at DST receiver input	1.4 dB nominal 2.9 dB maximum (end of life)
Acquisition and tracking rate	550 Hz/s at signal Level > −110 dBm
Tracking range	±250 kHz minimum
Tracking error	<1°/40 kHz at carrier level > −110 dBm
Capture range	±1.3 kHz at signal level > −120 dBm
5. Exciter parameters	
Frequency for coherent operation	880/749 times uplink frequency
Frequency for noncoherent operation	approximately $880F_1$
RF output power level	+12 dBm, nominal
Output Impedance	50 ± 5 ohms, nominal
Spurious signals	60 dB below the carrier
Modulation bandwidth	>40 MHz
Modulation index	Ranging: 3–9 dB carrier suppression Telemetry: 0–15 dB carrier suppression DOR: 0–1.1 dB carrier suppression
Modulation sensitivity	2 radians peak/volt peak
Modulation amplitude linearity	±2.5 radians at ±8% linearity
Modulation index stability	±10% over −20°C to +75°C
Residual phase noise	<2.5° rms in the coherent mode <2.8° rms in the noncoherent mode
Input-to-output carrier phase delay variation	<2.5 nsec over −10°C to +55°C
Differential phase delay variation	<1 nsec over −10°C to +55°C
Ranging phase delay variation	<22 nsec over −10°C to +55°C

range from −10°C to +55°C, respectively. The differential downlink carrier phase delay variation is to be less than 1 nsec over the same temperature range. The hardware must withstand 100-krad (silicon) total radiation dose.

III. TRANSPONDER

A. Block Diagram and Frequency Scheme

The DST functional block diagram and frequency-generation scheme are shown in Fig. 1. The receiver is implemented as a double-conversion superheterodyne phase-lock tracking receiver, with a fixed frequency second intermediate frequency (IF). The first local oscillator (LO) signal at $880F_1$ and the second LO signal at $131F_1 - F_2$ are generated by a dielectric resonator oscillator (DRO) [3] and a surface acoustic wave resonator oscillator (SRO), respectively. Both of these oscillators are phase locked to the $12F_1$ (114.75 MHz) voltage controlled oscillator (VCO). The $12F_1$ VCO is in turn phase locked to the uplink carrier. The SRO PLL consists of a SRO, a $\times 11$ multiplier, a $\div 6$ divider, two mixers, a $\div 2$ divider, and a phase detector. The $\times 11$ multiplier and $\div 6$ divider are used in the SRO PLL to generate the frequencies $132F_1$ and $2F_1$ from $12F_1$. The $2F_1$ and the reference oscillator output at $2F_2$ are applied to a mixer followed by a $\div 2$ divider to obtain a reference signal at $(F_1 + F_2)$ to the SRO PLL phase detector. The SRO output at $131F_1 - F_2$ and the $132F_1$ signals are applied to a mixer to obtain the second input signal at $(F_1 + F_2)$ to the SRO PLL phase detector. A $\times 73$ multiplier and a $\div 3$ divider are used in the DRO PLL to generate reference signals at $836F_1$ and $4F_1$, respectively. The first and second intermediate frequencies are at $131F_1$ (1252.6875 MHz) and F_2 (56.648 MHz), respectively. Coherent carrier automatic gain control (AGC) is employed in both of the IF sections to provide a constant signal plus noise at the carrier loop phase detector.

The coherent downlink carrier at $880F_1$ is provided by the LO DRO when the DST is operating in the coherent mode from the VCO. In the noncoherent mode, an $880F_1$ frequency is generated by the exciter DRO phase locked to the DST $12F_1$ auxiliary oscillator (AUX OSC) or the external USO. The noncoherent downlink signal is automatically selected by the receiver AGC function upon the absence of an uplink signal. The DST's $880F_1$ phase-modulated signal [4] provides drive for the redundant spacecraft power amplifiers.

Prior-Art in the Deep Space Transponder Technology: The NASA *S*-band transponder developed in the early seventies, has been the choice of past planetary missions. Full-up *S*/*X*-band dual frequency downlink capabilities have been demonstrated in Galileo and Magellan radios. The *S*-band downlink to *S*-band uplink frequency translation for coherent operation is 240/221. The phase lock receiver is a double-conversion superheterodyne type. The receiver $2F_1$ VCO is phase locked to the uplink carrier at $221F_1$ (2113.3125 MHz). The downlink carriers at $240F_1$ are generated by frequency multiplication from the $2F_1$ VCO for the coherent mode or from a USO for the noncoherent mode. The *S*-band downlink signal at $240F_1$ is generated by using frequency multipliers from the input drive frequency at $2F_1$. The phase modulation is applied at $30F_1$.

The Galileo Magellan radios utilize *S*-band transponders as the basic phase locked receiver with additional circuits that include an *X*/*S*-band downconverter in front of the *S*-band receiver and an *X*-band exciter.

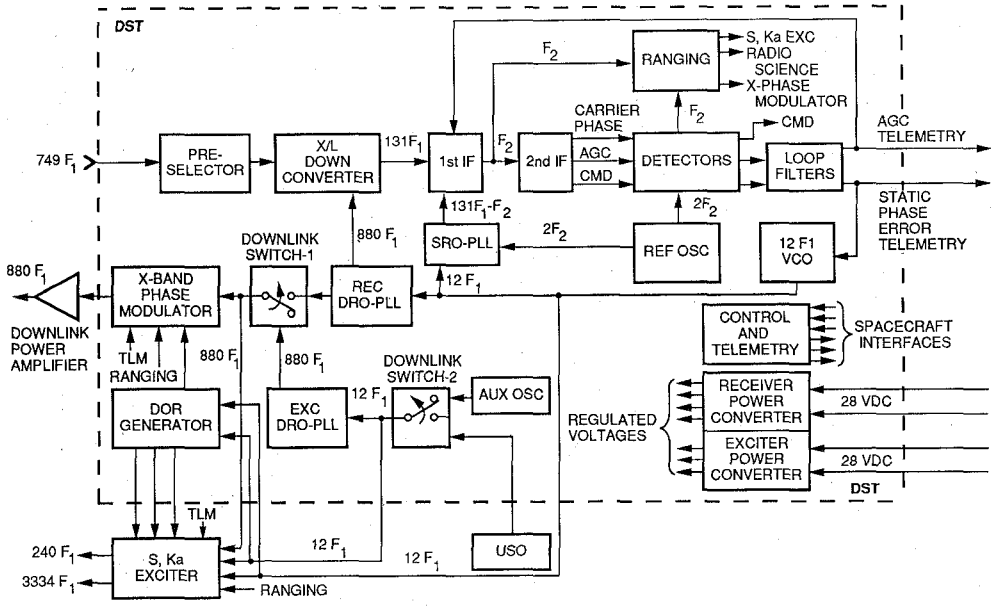

Fig. 1. Deep space transponder (DST) functional block diagram.

B. Automatic Phase Tracking Loop

An automatic phase tracking loop in the receiver is used to phase track the uplink carrier and to provide good dynamic response. The selection of the PLL bandwidth depends on the tracking threshold, phase noise, and dynamic performance of the receiver.

In the coherent mode, the $880F_1$ downlink signal generated in the DST exciter from the $12F_1$ VCO signal is phase coherent with $749F_1$ received signal. Phase coherence is accomplished by a automatic phase-lock loop (PLL) in the receiver. The receiver PLL transfer function is a type-I, second-order lowpass filter [5], [6]. The PLL design [5]–[7] is an involved iterative task and is usually a compromise between fast low-error tracking operation and noise response. The selection of the loop filter time constants (τ_1 and τ_2), the loop gain (K_V), and the noise equivalent predetection bandwidth (B_{LI}), depends on six relevant receiver performance requirements. The requirements are:

1) the steady-state tracking error less than or equal to 1° per 40 kHz offset at carrier levels greater than −110 dBm

2) the minimum acceptable signal-to-noise power ratio (SNR) in the carrier channel at the phase detector input equal to −25 dB

3) the minimum acquisition sweep rate at strong signal (> −110 dBm) equal to 550 Hz/sec

4) the damping factor at the theoretical threshold (−157.3 dBm) ranges from 0.4 to 0.6

5) the damping factor at 10 dB above the theoretical threshold ranges from 0.5 to 0.8

6) the two-sided loop noise bandwidth ($2B_{LO}$) at the theoretical threshold of 18 Hz

Using the above set of transponder performance requirements, the loop parameters τ_1, τ_2 and K_V are selected using PLL algorithm. Performance variations of the components over temperature and aging are considered in selecting the PLL designs. Table II lists these loop parameters and compares them for several transponders: NASA Standard, Galileo and Magellan.

C. Residual Phase Noise

In the coherent carrier mode, residual phase noise is defined for a noise-free received signal case. The phase noise on the downlink carrier signal consists primarily of contributions from the three phase-locked oscillators $12F_1$ VCO, SRO, and DRO used in the DST implementation. Individual phase noise power spectral density functions [8]–[10] for these contributors are used in a comprehensive computer program to predict the phase noise of the closed-loop receiver. Total residual phase noise in the output is the mean square sum of all noise sources. The predicted phase noise for the DST in the coherent mode is shown in Fig. 2. In the intervals between 5 Hz and 25 MHz on each side of the carrier, the root mean square (rms) phase noise is 0.448 degrees rms, which is well below the maximum allowable 2.5 degrees for coherent downlink. The dominant contributor to this rms phase noise is the $12F_1$ VCO; the remaining contributors are less than 10% of the VCO contribution. Predicted rms phase noise and Allan deviation [9] are compared to the specified values in Table III. The results of the analysis indicate that the coherent mode specifications will be met for both the rms phase noise and the Allan deviation. The receiver PLL band limits the VCO spectrum, thus providing the superior performance in the coherent mode.

D. Carrier Delay and Delay Variation

The phase variation associated with the temperature change of the transponder can be estimated by construct-

TABLE II
TRANSPONDER CARRIER TRACKING LOOP PARAMETER

Transponder	Design Parameter			Threshold Parameters			10 dB Above Threshold Parameters			Strong Signal (50 dB Above Threshold)			
	K_V/s	$\tau_1 s$	$\tau_2 s$	ζ_0	ω_{n0} rad/sec	$2B_{L_O}$ Hz	ζ_{10}	ω_{n10} rad/sec	$2B_{L_{10}}$ Hz	ζ_s	ω_{n_s} rad/sec	$2B_{L_s}$ Hz	$\Delta\dot{\omega}$ Hz/s
NST	1.44×10^7	2910	0.0833	0.68	16.2	17.0	1.20	28.7	40.3	2.92	70.3	211.4	392.4
NST + XSDC	4.88×10^7	2910	0.0833	1.90	45.8	92.5	3.27	78.4	262.3	5.39	129.5	704.0	1334.5
GLL	1.62×10^7	3732	0.0423	0.32	15.1	16.7	0.56	26.7	26.9	1.39	65.9	103.3	345.6
GLL + XSDC	5.73×10^7	3732	0.0423	0.74	34.8	37.5	1.29	61.1	90.7	2.62	123.9	335.4	1221.6
MAG	1.44×10^7	728	0.0208	0.42	40.5	41.0	0.74	70.7	76.2	1.46	140.6	229.0	1569.0
MAG + XSDC	4.88×10^7	728	0.0208	1.02	97.9	123.6	1.74	166.8	313.5	2.69	258.9	718.7	5334.0
DST	2.2×10^7	3556	0.0556	0.50	18.0	18.0	0.88	31.9	37.2	2.17	78.1	178.5	550.0

K_V = dc gain of phaselock loop (seconds^{-1})
τ_1 = time constant associated with open-loop pole (phase-lag) of the loop filter, (seconds)
τ_2 = time constant associated with open-loop zero (phase-lead) of the loop filter, (seconds)
ζ_0, ζ_{10}, ζ_s = PLL damping factor at threshold, 10 dB above threshold, and strong signal
ω_{n0}, ω_{n10}, ω_{n_s} = PLL natural frequency at threshold, 10 dB above threshold, and strong signal (radians/second)
$2B_{L_0}$, $2B_{L_{10}}$, $2B_{L_s}$ = PLL noise-equvalent bandwidth at threshold, 10 dB above threshold, and strong signal (Hz)
$\Delta\dot{\omega}$ = PLL aquisition and tracking rate at strong signal (Hz/s)
NST = NASA standard deep space transponder (*S*-band)
GLL = Galileo transponder (*S*-band)
MAG = Magellan transponder (*S*-band)
DST = Deep space transponder (*X*-band design)
XSDC = External *X*-band to *S*-band downconverter

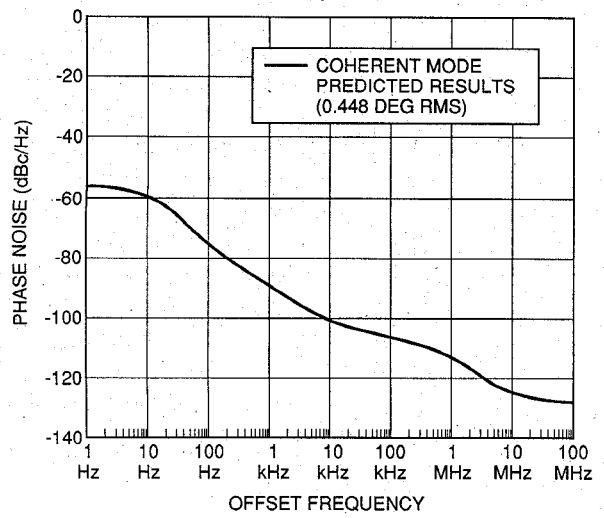

Fig. 2. Deep space transponder (DST) 880F$_1$ coherent mode phase noise.

TABLE III
TRANSPONDER COHERENT MODE PREDICTED RMS PHASE NOISE AND ALLAN DEVIATION

	Predicted Output	Specification
RMS Phase Noise (Degrees RMS)	0.448	2.5 (5 Hz to 25 MHz)
Allan Deviation: (Integration Time)		
0.01 sec	2.6×10^{-11}	3×10^{-11}
1.0 sec	2.6×10^{-13}	1.2×10^{-12}
1000 sec	2.4×10^{-15}	5×10^{-15}

ing a model from the block diagram. The analysis assumes that the frequency multipliers are major contributors of the phase delay variation with temperature. The contribution for each multiplier is assumed to be three degrees of phase per degree Celsius. The estimated value of the DST carrier phase delay variations from input to output is equal to 0.075 nsec over the temperature range from $-10°C$ to $+55°C$. The predicted carrier delay data indicates that DST satisfies the requirement of maximum allowable delay variations equal to 2.5 nsec.

IV. TRANSPONDER EXPERIMENTAL RESULTS

A breadboard DST *X*-band receiver and exciter shown in Fig. 1 (without *S*-band and *Ka*-band exciters) was implemented and performance characterization accomplished. The evaluation measurements include receiver tracking threshold sensitivity, static phase errors for *X*-band uplink frequency offset, swept acquisition characteristics, and AGC versus uplink signal level. All measurements were made at a room temperature (25°C). The theoretical equations used for the calculation of carrier tracking threshold and phase jitter are given in the Appendix. The measured tracking threshold sensitivity at the receiver best lock frequency (approximately channel center) is -158 dBm, which is in good agreement with the design threshold value of -157.3 dBm [Appendix: (A1)]. The measured receiver threshold characteristics show good correlation with expected performance [Appendix (A2) and (A6)] over the tracking range as shown in Fig. 3. The receiver acquisition characteristics were measured

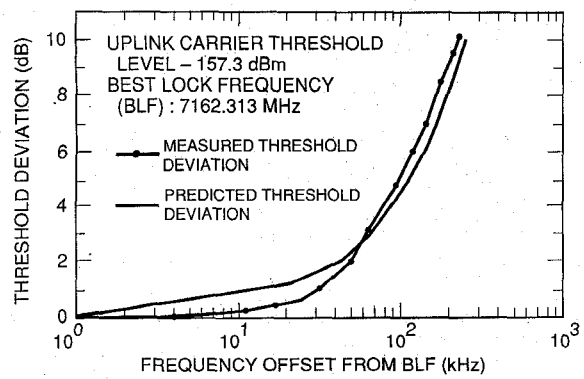

Fig. 3. Deep space transponder (DST) carrier tracking threshold versus offset frequency.

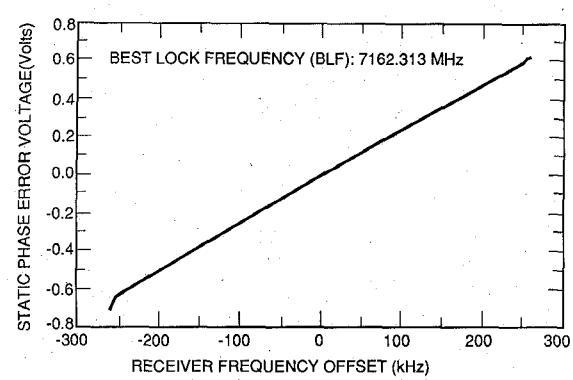

Fig. 4. Deep space transponder (DST) static phase error voltage versus offset frequency.

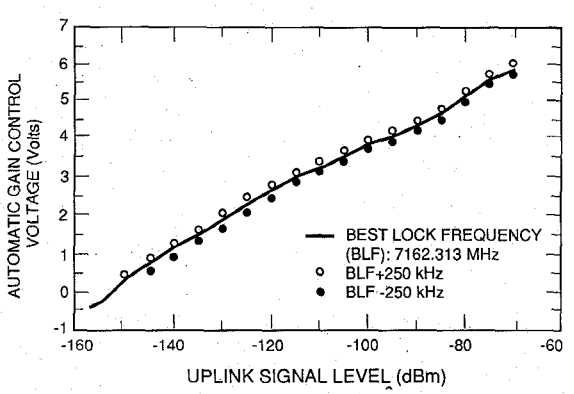

Fig. 5. Deep space transponder (DST) automatic gain control (AGC) voltage versus uplink signal level.

at an input signal level of −110 dBm. The measured values for tracking range and tracking rate are ±270 kHz at design center frequency, and 800 Hz/sec, respectively, and meet the specified requirements (Table I). Fig. 4 shows a linear relationship for the static phase error voltage versus uplink frequency offset over the receiver tracking range. The AGC loop-filter amplifier-output voltage controls the gain in the first and second intermediate (IF) amplifiers. The AGC voltage versus uplink signal level at the best lock frequency and at frequency offsets of ±250 kHz from BLF are shown in Fig. 5. As the receiver input signal varies from a strong signal level (−70 dBm) to the threshold level, the AGC control voltage varies approxi-

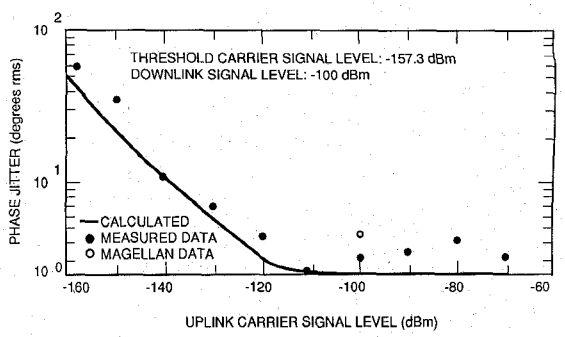

Fig. 6. Deep space transponder (DST) phase jitter versus uplink signal level.

mately linearly (better than 5% linearity). No receiver false-lock or self-lock resulted during the test phase.

A comparison of measured to calculated phase jitter [1], [5], [6], [7] characteristics [Appendix: (A7)] as a function of receiver uplink signal level is shown in Fig. 6. The measured phase jitter values for the breadboard DST and Magellan transponders at the same uplink signal level of −100 dBm are equal to 3.03° rms and 3.98° rms, respectively.

V. Conclusion

Design concepts and system architecture for a high performance *X*-band (7162 MHz/8415 MHz) DST for deep space spacecraft applications have been presented. The DST has been successfully breadboarded and evaluated. New technologies such as a dielectric resonator oscillator, *X*-band (8415 MHz) phase modulator, and surface acoustic wave resonator oscillator have been integrated into the design. The Telecommunication Development Laboratory measurements on the breadboard DST achieved a threshold level of −158 dBm with a dynamic range of 88 dB, and excellent acquisition and tracking characteristics. The measured tracking receiver threshold and phase jitter data are in good agreement with the predicted characteristics. The Jet Propulsion Laboratory breadboard *X*-band DST design and evaluation has demonstrated a basic model configuration for implementation of future deep-space transponders.

Acknowledgment

The research described in this paper was performed by the Jet Propulsion Laboratory, California Institute of Technology, under contract with the National Aeronautics and Space Administration. The authors gratefully acknowledge the valuable support by John T. Meysenburg for breadboard fabrication and testing, Peter W. Kinman for phase delay calculations, and Keith Siemsen of Motorola (Strategic Electronics Division, Chandler, AZ) for phase noise calculations.

Appendix

The equations used to calculate carrier tracking threshold and phase jitter data are presented in this appendix.

1. Carrier Tracking Threshold of a Phase-Lock Loop Receiver

The carrier tracking threshold of a phase-locked loop (PLL) receiver [1], [5], [6], [7] is defined as the minimum uplink signal required to maintain lock at any given offset from best lock frequency. It is a measure of an important limitation on spacecraft receiver performance.

The worst case carrier tracking threshold signal level (S_0) at the transponder input port and at the best lock frequency (BLF) is determined from the following equation:

$$S_0 = kT_0F(2B_{LO})L \tag{A1}$$

where S_0 is the receiver input signal power level for tracking threshold at receiver BLF, k is Boltzmann's constant, T_0 is the reference system temperature, F is the receiver noise figure at the transponder input, $2B_{LO}$ is the two-sided noise-equivalent receiver carrier tracking loop bandwidth at threshold, and L is the receiver carrier channel loss. The calculated value of the worst case receiver carrier tracking threshold is equal to -157.5 dBm for a $2B_{LO}$ of 18 Hz, channel loss of 1 dB, and noise figure of 2.9 dB at 290 K.

The PLL receiver limiter suppression factor [1], [5], [6], α, is given by

$$\alpha = \frac{1}{\sqrt{1 + \dfrac{4B_{LI}S_0}{\pi 2B_{LO}S}}} \tag{A2}$$

with S is the receiver input signal power level, and B_{LI} is the noise-equivalent predetection bandwidth.

The performance of a PLL receiver at its tracking threshold is nonlinear and not easily modeled. An empirical approach was taken to the derivation of equations to predict the receiver behavior at the tracking threshold. The assumption was that the tracking threshold phase offset at the loop phase detector cannot exceed an angle equal to one radian minus the rms value of the noise in the loop. At BLF, there is one radian of noise and the phase offset cannot exceed zero, however when the noise is reduced by increasing the signal level by 25% of one radian, the maximum phase offset at the signal level is 0.25 radians.

In the region near tracking threshold, the phase offset, θ_e, at the PLL phase detector can be estimated from the empirical equation

$$\theta_e = 1 - \frac{\alpha_o}{\alpha} \tag{A3}$$

where α_o is the limiter suppression factor at carrier threshold given by

$$\alpha_o = \sqrt{\frac{\pi 2B_{LO}}{4B_{LI}}}. \tag{A4}$$

The phase detector output voltage is given by an empirical equation

$$V_c = \alpha \sin(\theta_e)\cos(\theta_e). \tag{A5}$$

The frequency offset at X-band this voltage can produce is

$$\Delta f = \frac{1}{2\pi} V_c K_V \tag{A6}$$

where K_V is the dc gain of the PLL.

Equations (A2), (A3), and (A4) are used to predict the carrier tracking threshold as a function of the offset frequency (Δf) from BLF.

2. Phase Jitter Calculations

The root mean square (rms) value of the PLL loop phase jitter [1], [5], [6], [7] at a given receiver input signal level is calculated from

$$J_p = \sqrt{\frac{S_0B_L}{S2B_{LO}}}. \tag{A7}$$

The one-sided noise-equivalent loop bandwidth, B_L, in (A7) is given by

$$B_L = \frac{\alpha K_V}{4(1 + \tau_2\alpha K_V)}\left[1 + \frac{\tau_2^2\alpha K_V}{\tau_1}\right] \tag{A8}$$

where τ_1 is the time constant associated with the open-loop pole (phase lag) of the loop filter, and τ_2 is the time constant associated with the open-loop zero (phase lead) of the loop filter.

REFERENCES

[1] J. H. Yuen, *Deep Space Telecommunications System Engineering*. New York: Plenum, 1983.

[2] N. R. Mysoor, J. D. Perret, and A. W. Kermode, "Design concepts and performance of NASA X-band (7162 MHz/8415 MHz) transponder for deep-space spacecraft applications," *TDA Progress Report 42-104*, vol. Oct.-Dec. 1990, Jet Propulsion Laboratory, Pasadena, CA, pp. 247–256, Feb. 15, 1991.

[3] N. R. Mysoor, "An electronically tuned, stable 8415 MHz dielectric resonator FET oscillator for space applications," *Proc. IEEE 1990 Aerospace Applications Conf.*, Feb. 5–9, 1990, Vail, CO.

[4] N. R. Mysoor, "A low-loss linear analog phase modulator for 8415 MHz transponder applications," *TDA Progress Report 42-96* vol. Oct.-Dec. 1988, Jet Propulsion Laboratory, Pasadena, CA, pp. 172–178, Feb. 15, 1989.

[5] F. M. Gardner, *Phaselock Techniques*. New York: Wiley, 1979.

[6] A. Blanchard, *Phase-Locked-Loops: Applications to Coherent Receiver Design*. New York: Wiley, 1976.

[7] J. P. Frazier and J. Page, "Phase-lock loop frequency acquisition study," *IRE Trans. Set-8*, pp. 210–227, Sept. 1962.

[8] D. B. Leeson, "A simple model of feedback oscillator noise spectrum," *Proc. IEEE*, vol. 54, pp. 329–330, Feb. 1966.

[9] J. A. Barnes, A. R. Chi, and L. S. Cutler, *Characterization of Frequency Stability*, National Bureau of Standards Technical Note 394, Washington, DC, National Bureau of Standards, Oct. 1970.

[10] D. W. Allan, "Time and frequency (time-domain) characterization, estimation and prediction of precision clocks and oscillators," *IEEE Trans. Ultrason. Ferroelec. Freq. Contr.*, Vol. UFFC-34, no. 6, pp. 647–654, Nov. 1987.

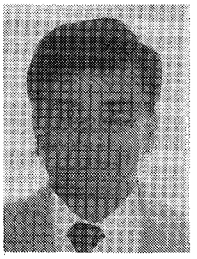

Narayan R. Mysoor (S'70–M'78–SM'91) received the B.S.E.E. degree in electrical engineering from Bangalore University, India, in 1969, and the M.S.E.E. and Ph.D. degrees in electrical engineering from the University of Delaware in 1974 and 1978, respectively.

He joined the Electrical and Computer Engineering faculty at California State Polytechnic University, Pomona, in 1978, where he presently holds the rank of Professor. He joined the Technical Staff at Jet Propulsion Laboratory as a part time faculty employee in 1985. He is currently engaged in the development of microwave circuits, MMICs, and microwave photonics for Advanced Deep Space Transponders. His main fields of interest include microwave engineering, microwave/optical communications, fiber-optics, photonics, and semiconductor devices.

Dr. Mysoor is a Registered Professional Engineer in the State of California. He has authored over 30 technical publications. He has been the recipient of the Cal Poly Faculty Service Award, and the NASA Innovative Tech-Brief Award. He is a member of Eta Kappa Nu.

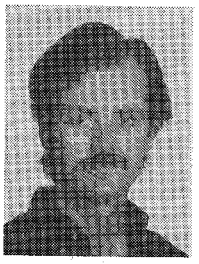

Jonathan D. Perret (M'82) received the B.S. degree in electrical engineering from California State Polytechnic University, Pomona, in 1980, and M.S. degree in Electrical Engineering from California State University Los Angeles in 1982.

In 1980, he joined the Jet Propulsion Laboratory as a Telecommunications Hardware Engineer. He became a Technical Supervisor of the Radio Frequency Subsystems Group in 1991. During that time he has contributed to the technical development of advanced technology and hardware for spacecraft applications. His contributions to the flight products include an experimental Convolutional Encoder for Galileo, a Command Detector Unit for Mars Observer, and the Deep-Space Transponder. He is currently developing the Radio Frequency Subsystems for the CRAF/Cassini project.

Arthur W. Kermode (M'62) received the B.S. degree in electrical engineering from California State Polytechnic University, Pomona, in 1962.

Since 1984 he has been the Supervisor of the Spacecraft Transponder Development Group and has been with Jet Propulsion Laboratory for 25 years. During the time he has contributed to the technical development and management of advanced technology and hardware for spacecraft applications. Flight development products include the experimental *X*-band downconverter Subsystems that were utilized on both Galileo and Magellan spacecraft, an experimental Convolution Encoder-2 for Galileo, and a breadboard *Ka*-band exciter for CRAF/Cassini. Current hardware developments include the *X*-band deep Space Transponder, Command Detector Unit, Telemetry Modulator Control Unit and the radio frequency subsystems for CRAF and Cassini missions.